HHS Public Access

Author manuscript

*Acc Chem Res*. Author manuscript; available in PMC 2018 December 19.

Published in final edited form as:

*Acc Chem Res*. 2017 December 19; 50(12): 2915–2924. doi:10.1021/acs.accounts.7b00305.

# Molecular Tension Probes for Imaging Forces at the Cell Surface

**Yang Liu**[1], **Kornelia Galior**[1], **Victor Pui-Yan Ma**[1], and **Khalid Salaita**[1,2,*]

[1]Department of Chemistry, Emory University, Atlanta, GA 30322, USA

[2]Wallace H. Coulter Department of Biomedical Engineering, Georgia Institute of Technology and Emory University, Atlanta, GA 30332, USA

## Conspectus:

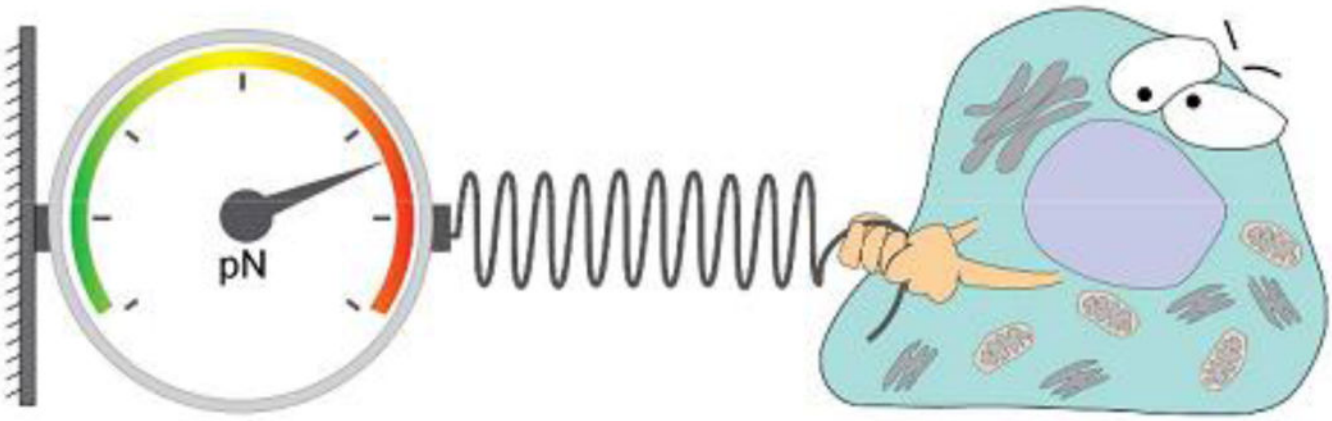


Mechanical forces are essential for a variety of biological processes ranging from transcription and translation to cell adhesion, migration and differentiation. Through the activation of mechanosensitive signaling pathways, cells sense and respond to physical stimuli from the surrounding environment, a process widely known as mechanotransduction. At the cell membrane, many signaling receptors, such as integrins, cadherins and T or B-cell receptors, bind to their ligands on the surface of adjacent cells or the extracellular matrix (ECM) to mediate mechanotransduction. Upon ligation, these receptor-ligand bonds transmit piconewton (pN) mechanical forces that are generated, in part, by the cytoskeleton. Importantly, these forces expose cryptic sites within mechanosensitive proteins and modulate the binding kinetics (on/off rate) of receptor-ligand complexes to further fine-tune mechanotransduction and the corresponding cell behavior.

Over the past three decades, two categories of methods have been developed to measure cell receptor forces. The first class is traction force microscopy (TFM) and micro-post array detectors (mPADs). In these methods, cells are cultured on elastic polymers or microstructures that deform under mechanical forces. The second category of techniques is single molecule force spectroscopy (SMFS) including atomic force microscopy (AFM), optical/magnetic tweezers and biomembrane force probe (BFP). In SMFS, experimenters apply external forces to probe the mechanics of

*Corresponding Author: k.salaita@emory.edu.

The authors declare no competing financial interest

individual cells or single receptor-ligand complexes, serially, one bond at a time. Although these techniques are powerful, the limited throughput of SMFS and the nN force sensitivity of TFM have hindered further elucidation of molecular mechanisms of mechanotransduction. In this account, we introduce the recent advent of molecular tension fluorescence microscopy (MTFM) as an emerging tool for molecular imaging of receptor mechanics in living cells. MTFM probes are composed of an extendable linker, such as polymer, oligonucleotide, or protein, and flanked by a fluorophore and quencher. By measuring the fluorescence emission of immobilized MTFM probes, one can infer the extension of the linker and the externally applied force. Thus, MTFM combines aspects of TFM and SMFS to optically report receptor forces across the entire cell surface with pN sensitivity. Specifically, we provide an in-depth review of MTFM probe design, which includes the extendable “spring”, spectroscopic ruler, surface immobilization chemistry, and ligand design strategies. We also demonstrate the strengths and weaknesses of different versions of MTFM probes by discussing case studies involving the pN forces involved in EGFR, integrin and T-cell receptor signaling pathways. Lastly, we present a brief future outlook, primarily from a chemists’ perspective, on the challenges and opportunities for the design of next generation MTFM probes.

## 1. Introduction

Living systems are exquisitely sensitive to mechanical cues that influence a broad range of processes such as biofilm formation,[1] embryonic development,[2] immune response,[3] wound healing,[4] cell proliferation and differentiation.[5] Akin to the biochemical exchange of information, mechanical interactions constantly and dynamically occur among neighboring cells or between cells and their extracellular matrix (ECM).[6] Therefore, it is not surprising that almost all cells have evolved the ability to detect and convert mechanical information into biochemical signals, a process widely known as mechanotransduction.

The cellular cytoskeleton is the main force generating machinery within cell and is driven by the collective activity of motor proteins acting on the filamentous scaffolds of actin and microtubules. Given that a cell is constantly sensing the mechanical properties of its external environment, many mechanotransduction processes are mediated by cell surface receptors interacting with the cytoskeleton. For example, integrins are a class of heterodimeric α transmembrane receptors that spontaneously assemble into focal adhesion (FA) assemblies and transmit cellular forces bi-directionally to their ECM.[7] Several other surface receptors, such as cadherins,[8] T or B cell receptors,[9,10] Notch[11] and many receptor tyrosine kinases (RTKs)[12] also transmit forces to their cognate ligands and their activation pathways are mechanosensitive.

One mechanism for the mechanical regulation of a biochemical signal transduction pathway involves modulating the kinetics of protein-protein interactions as a function of force, which usually accelerates the dissociation of a bond.[13] A bond that displays reduced dissociation rates when experiencing a mechanical force is counter-intuitive, but is observed in a number of receptors and is described as a catch bond.[14,15] Forces can also change the equilibrium distribution for a two-state system separated by an activation barrier.[16] Figure 1 shows a simplified model (Bell model) to demonstrate the role of forces in driving reactions. An

external force ($F$) changes the free energy landscape of reaction from $G^0$ (black curve) to $G^0-F\Delta x$ (red curve), and also lowers the energy barrier $\Delta G^{\ddagger}$ and the $G^0$ of state B (Figure 1).[17,18] Consequently, the reaction rate ($k_{forward}$) and the population distribution between states A and B are modified. Therefore, it is critical to develop tools for force measurement in order to better understand how mechanics influences binding kinetics, shifting equilibrium distributions of proteins and ultimately controlling signaling pathways within the context of a living cell.

In the past three decades, a number of innovative techniques have been developed for measuring forces in living cells. The first class of techniques focused on measuring the deformation of soft polymer networks, such as traction force microscopy (TFM) (Figure 2A, left).[19] Although TFM is widely used by the biomechanics research community, the method is only sensitive to forces at the nN level, yielding a spatial resolution and force sensitivity that is orders of magnitude coarser than the forces applied by individual receptors (Table 1).

A second general strategy for measuring forces is single molecule force spectroscopy (SMFS) that includes atomic force microscopy (AFM),[20] optical/magnetic tweezer[21] and biomembrane force probe (BFP)[15] (Figure 2A, right). SMFS allows the measurement of forces ranging from below 1 pN to several nN, which provides an appropriate means to investigate the mechanical response of single biomolecules with high sensitivity. However, SMFS methods are low throughput and interrogate only one bond at a time, thus failing to capture the mechanics of a whole cell or to fully activate surface receptors that require clustering in their physiological conditions.

In 2011, our lab pioneered the development of molecular tension fluorescence microscopy (MTFM) where a probe comprised of a fluorophore-quencher pair separated by a molecular “spring” is immobilized onto a surface (Figure 2B).[22] By using fluorescence microscopy, one can visualize probe extension events across the entire cell surface, thus combining the high-throughput of TFM with the pN sensitivity of SMFS (Table 1 and Figure 2B).[23] In contrast to the cross-linked nature of TFM substrates, each MTFM probe consists of one elastic molecule that independently reports the mechanical forces generated by its bound receptor. With this strategy, one can map the tension applied by cell receptors with molecular specificity, submicron spatial resolution, millisecond temporal resolution and pN force sensitivity (Table 1). Ongoing developments in fluorescence microscopy will further push the limits of MTFM.

The purpose of this Account is to present our recent efforts in developing MTFM probes for visualizing cellular forces. We will first discuss the general design principles and several important components of the synthetic probes, and then showcase recent biological applications using these probes. Finally, we will briefly discuss the technical limitations and potential future improvements to MTFM.

## 2. Guidelines for the design of immobilized tension probes

Typically, MTFM probes consist of a flexible linker flanked by a fluorophore-quencher pair.[22] The probe is decorated with a biological ligand at one terminus and is immobilized to the

substrate through the other terminus. The substrate can be a conventional glass coverslip[22] or supported lipid membrane.[24] In the resting state, MTFM probes adopt a relaxed or closed conformation in which the fluorophore is strongly quenched due to proximity to the quencher. When forces are transmitted through the ligand-receptor complex, tension stretches the linker extending it from its resting conformation, and thus increasing the distance between the two dyes and restoring fluorescence. To design an efficient MTFM sensor, a few general rules are critical (Figure 2B). First, the extendable linker needs a mechanical resistance that is matched to the pN forces under investigation; second, the extension of the linker should exceed the quenching distance of the fluorophore/quencher pair to maximize sensitivity; third, the quenching efficiency of the dye should be maximized when the probe is at resting; finally, individual MTFM probes must be immobilized onto the substrate through a stable chemical bond to sustain receptor forces without rupturing. Note that we have also developed new strategies to convert the extension of the linker into a catalytically amplified signal, thus enhancing the potential sensitivity of MTFM.[25]

## 3. Selecting the key components of immobilized tension probes

### 3.1 Mechanical “spring”

Typically, unfolding proteins, peptides, or oligonucleotides involves rupturing non-covalent bonds requiring energy levels on the order of 1–100 kcal/mol. For example, the $\Delta G$ of unfolding a typical RNA hairpin is ~35 kcal/mol[26] (blue area, Figure 3A). Note that 1 kcal/mol is equivalent to ~6.9 pN●nm. Therefore, we can estimate the rupture force of an RNA hairpin at ~ 12 pN (assuming a 20 nm extension). Several covalent mechanophores have been reported[27], however, these types of probes are sensitive to forces of hundreds or thousands of pN (100–1000 kcal/mol). Other examples of optical force probes include semiconductor tetrapod crystals that deform due to stress[28] (green and red area, Figure 3A). Such probes are insensitive to the molecular forces (1–100 pN) that mediate mechanotransduction pathways in biology.

In MTFM, different molecules have been used as the spring element in tension probes. Here, we classify these molecules into two categories: (i) switch-like springs with defined secondary structure such as DNA hairpins and protein domains; (ii) entropic springs with a random coil conformation such as polyethylene glycol (PEG),[22] single-stranded DNA[29] and elastic polypeptide (EP)[30]. In the first category, the molecular spring adopts a defined structural motif (secondary or tertiary structure) such as a DNA stem loop hairpin[31] and α-helical or β-sheet polypeptide.[32,33] In the case of DNA hairpins, the stability ($\Delta G$) is a primary determinant of the magnitude of forces required for mechanical unfolding (eq. 1),[34,35]

$$F_{1/2} \approx \frac{\Delta G_{fold} + \Delta G_{stretch}}{\Delta x} \quad 1$$

where $F_{1/2}$ is the equilibrium force that leads to a 50% probability of unfolding, $\Delta G_{fold}$ is the free energy of unfolding the hairpin at $F = 0$, $\Delta G_{stretch}$ is the free energy of stretching ssDNA

from $F = 0$ to $F = F_{1/2}$, and $\Delta x$ is the hairpin displacement needed for unfolding.[31,36] The probability of unfolding as a function of $F$ is defined in eq. 2,

$$P_u(F) \approx \left\{1 + \exp\left[\frac{(F_{1/2} - F) \times \Delta x}{k_B T}\right]\right\}^{-1} \quad 2$$

where $k_B$ is the Boltzmann constant and T is the temperature. Notably, mechanical unfolding of these highly ordered structures is cooperative, displaying a "digital" response to external forces within a narrow window (*i.e.* conformational change is only observed when the force applied approaches the force threshold for unfolding) (Figure 3B).

The second category of springs includes polymer chains that adopt random conformations at zero force.[37] In contrast, these entropic springs yield an "analogue" response to forces where their extension proportionally responds to the magnitude of applied force (Figure 3C). For polymers such as PEG, it has been both theoretically and experimentally shown that the force-extension curve of these springs follows the worm-like chain (WLC) model (eq. 3),[38]

$$F = \frac{k_B T}{P}\left\{\frac{1}{4}\left(1 - \frac{x}{L_0}\right)^{-2} - \frac{1}{4} + \frac{x}{L_0}\right\} \quad 3$$

where $P$, $L_0$ and $x$ are the persistence length, contour length and the extension of the polymer chain, respectively. Based on this relationship, the dynamic force range of PEG-based springs solely depends on the contour length ($L_0$) of the polymer (*i.e.* $M_w$ of polymer) and the forces experienced by these polymers can be estimated by measuring their extension ($x$).

### 3.2 Spectroscopic rulers

To date, the spectroscopic ruler utilized in MTFM is often based on energy transfer between the fluorophore and quencher. Common resonance energy transfer mechanisms are fluorescence resonance energy transfer (FRET)[22] and nanometal surface energy transfer (NSET).[39] Contact (static) quenching is also employed frequently in DNA-based probes.[40]

In both FRET and NSET, the emission spectrum of the donor significantly overlaps with the absorption wavelengths of the quencher so that the energy of an excited donor is efficiently transferred to a nearby acceptor in a distance-dependent fashion. To unify these two mechanisms, the FRET/NSET efficiency ($E$) as a function of distance (r) has been mathematically described in one general equation (eq. 4),

$$E = \frac{1}{1 + \left(\frac{r}{R}\right)^n} \quad 4$$

where $r$ is the actual distance between the donor/quencher pair and constant $R$ is the distance at which the energy transfer efficiency is 50%. The FRET efficiency is governed by an inverse sixth power law ($n = 6$), while $R$ depends on the spectral overlap of the FRET pair. Here, a small $R$ (typically 4–7 nm) limits the detection of FRET signals within a short range of $r$ values (1–10 nm). However, in NSET, the donor dipole is strongly quenched by multiple dipoles presented on the surface of a gold nanoparticle rather than a single dipole, thus affording NSET with unique quenching capabilities.[41] First, the distance-dependent NSET efficiency follows an inverse fourth power law ($n = 4$), which yields a wider range of $r$ values for energy transfer than that of FRET (Figure 3C and D). Second, the $R$ for NSET is highly tunable depending on the nanoparticle size and the degree of spectral overlap between the AuNP and dye (Figure 3D). Typically, larger nanoparticles and more spectral overlap provide effective energy transfer at longer distances (>20 nm).[42]

As a rule of thumb, the choice of the quenching mechanism should always be considered along with the mechanical properties of the spring to ensure that the fluorophore is maximally quenched at zero force condition. For example, unfolding of a DNA hairpin probe labeled with the Cy3B/Black Hole Quencher (BHQ) pair leads to a 20-fold increase in fluorescence intensity (Figure 3E).[31] For “analogue” probes employing FRET or NSET, $R$ should match ~ half of the contour length of the polymer linker, such that the polymer extension leads to significant recovery of donor fluorescence. For example, FRET has been successfully used to monitor the dynamic conformational change of $PEG_{24}$ whose contour length ($L_0 = 8.4$ nm) falls within the working distance of typical dye-quencher pairs (Figure 3E).[22] However, in the case of longer springs, such as $PEG_{80}$ ($L_0 = 28.0$ nm), the change in FRET becomes negligible beyond the initial 10 nm extension (Figure 3C), and NSET ($R$ value > 15 nm) is preferred since it provides larger quenching distances and generates a 10-fold enhancement in fluorescence intensity (Figure 3C and E).[39]

### 3.3 Immobilization strategies

To visualize cell forces mediated by surface receptors, MTFM probes must be immobilized onto a substrate. Toward this end, an ideal immobilization strategy should be (i) chemically stable against the biological media and benign to all elements of the MTFM probe; (ii) physically robust to withstand mechanical dissociation over the timescale of an experiment; (iii) highly reproducible and facile to maintain a fixed average density of probes the substrate.

Thus far, three common coupling strategies have been used to graft MTFM probes onto surfaces. The first is affinity binding through which biotinylated probes are bound to streptavidin-modified substrates with high affinity ($K_d = 10^{-13}$ M).[43] The second strategy utilizes chemisorption, where thiolated probes are self-assembled onto a gold surface *via* the formation of gold-sulfur bonds.[25] This coupling provides not only high grafting density but also a semi-covalent linkage stronger than most other non-covalent bonds. In the third strategy, MTFM probes are covalently immobilized to a substrate via covalent coupling using efficient chemical or enzymatic reactions such as the “click” cycloaddition reaction[44] and halo-tag ligation.[45]

### 3.4 Ligand selection and conjugation

The choice of the ligand in the MTFM probes is very important as it dictates the specificity of ligand-receptor interaction, and hence the specificity of the tension signal reported. For instance, the RGD peptide motif can bind multiple integrin subtypes,[3146] whereas a specific peptide-MHC ligand only binds a single TCR.[15,47] Control experiments are often needed to test the specificity of the MTFM response. For example, if treatment with a blocking antibody that targets the receptor of interest abolishes the tension signal, then one can conclude that this tension signal is mediated through a specific receptor. [32]

In the case of chemically synthesized MTFM probes, the ligand can be directly conjugated to the molecular spring through efficient covalent coupling reactions such as native chemical ligation,[44] SMCC cross-coupling[48,49] and azide-alkyne cycloaddition reaction.[31] This strategy is ideal for peptide based ligands. In contrast, larger protein ligands are linked to the probes by affinity coupling, such as biotin-streptavidin interaction[9] and protein A/G-Fc interaction.[50] This interaction is not sufficiently stable to withstand high magnitude of forces such as those applied by integrins. However, weaker and more transient forces such as those applied by Notch receptors[11,50] and TCRs[9] are amenable to non-covalent conjugation. For recombinant MTFM probes, the ligand of interest can be directly engineered at the terminus of the protein spring.[32]

## 4. Biological applications of immobilized tension probes

### PEG-based Tension Probes

The first generation of PEG-based MTFM probes were engineered to report the mechanical forces associated with the endocytosis of epidermal growth factor receptor (EGFR),[22] which is known to broadly regulate cell survival, proliferation and differentiation (Figure 4A). Upon EGFR engagement, punctate force signals were detected and found to be associated with clathrin recruitment. Following this success, a similar PEG probe was developed to study integrin-mediated forces.[43] To this end, the biological ligand of the probe was modified with a cyclic RGD peptide, which has high affinity to the $\alpha_v\beta_3$ and $\alpha_5\beta_1$ integrins. [46] Unexpectedly, integrin receptors exerted forces sufficient to dissociate streptavidin-biotin complexes, the highest non-covalent interaction in nature. [43]

To address biotin-streptavidin dissociation, a gold nanoparticle (AuNP) based MTFM sensor was created to image integrin-mediated forces with up to 10-fold fluorescence increase (Figure 4B).[39] In this design, the MTFM sensor was immobilized to an AuNP surface through the formation of Au-thiol bond which ruptures at ~0.6–1 nN.[51] In addition, we combined AuNP-based MTFM with block copolymer micelle nanolithography (BCMN) to fabricate substrates with arrays of precisely spaced tension probes to investigate the impact of receptor nanoclustering on its force transmission.[52] This patterned MTFM strategy represents the first report of simultaneously measuring pN receptor forces while controlling receptor nanoclustering, which regulates surface receptors. We found that a critical ligand spacing (< 60 nm) is required to sustain high integrin forces that are pivotal in focal adhesion maturation, while loosely spaced ligand arrays (> 100 nm) destabilized FA formation and resulted in lower magnitudes of integrin forces. These experiments provide

the first mechanical insights into the role of integrin clustering during FA formation and we postulate that the cellular mechanism of sensing nanoscale ligand spacing is force-mediated.

## DNA-based sensor

With the aim of more precisely measuring integrin receptor tension, our lab and the Chen lab developed a new class of molecular tension probes, which employ DNA hairpins as a "switch" element, for imaging integrin generated tension during focal adhesion formation (Figure 5A).[31,49] By tuning the GC content in the stem region of a hairpin probe, a library of probes with $F_{1/2}$ (force required to unzip 50% of the probes) ranging from 4.7−19.3 pN was prepared (Figure 5C). When cells apply force greater than $F_{1/2}$, the probes are unfolded thereby separating fluorophore-quencher pair and resulting in a 20-fold increase in fluorescence.

Subsequently, we combined the DNA hairpin probe with the gold nanoparticle-based probes to provide the first pN tension maps of individual TCR-pMHC complexes (Figure 5B).[9] Dual quenching by the AuNP and molecular quencher provided a 100-fold increase in signal upon hairpin unfolding, affording the highest sensitivity of tension probes to-date. This sensitivity is essential given the transient nature and the limited number of TCR-pMHC antigens sufficient to activate T cells. We showed that naïve T cells harness cytoskeletal coupling to transmit force to their TCR-ligand complexes in a narrow range of 12–19 pN. More importantly, T cells display a dampened and poorly specific response to antigen agonists when TCR forces are chemically abolished or physically "filtered" to a level below ~12 pN using mechanically labile DNA tethers, suggesting a biophysical mechanism of antigen discrimination at pN resolution. Importantly, the DNA-AuNP sensor has been further integrated into a fluid lipid bilayer system. As a result, we showed that pN forces were sustained within TCR-mediated microclusters and during the formation of central supramolecular activation clusters (cSMAC).[24]

## Protein-based sensor

Given that integrin-mediated forces lead to DNA hairpin unfolding, DNA duplex unzipping, and biotin-streptavidin dissociation, we challenged integrins with protein based MTFM probes, which are potentially more mechanically stable. These probes were comprised of the immunoglobulin 27$^{th}$ (I27) domain of cardiac titin flanked with a fluorophore and gold nanoparticle (Figure 6).[32] AFM experiments suggested that unfolding of I27 requires a threshold force of >100 pN.[56] Accordingly, we created a series of I27 based tension probes displaying either RGD polypeptide or recombinant fibronectin 9–10$^{th}$ protein domains containing both RGD and the PHSRN synergy site (Figure 6A). Surprisingly, we found that integrin-mediated forces unfold the I27 domain and superfolder GFP with minutes of cell engagement, suggesting that integrin forces may exceed 30 pN. Note that the mechanical loading rate of a integrin receptor within focal adhesions is unknown and limits our ability to precisely determine the magnitude of the applied tension. Next, a covalent disulfide bridge that resists pN mechanical unfolding was engineered within the I27 to "clamp" the probe (Figure 6B and C). Incubation with a reducing agent DTT initiates SH exchange, thus unclamping I27 at a rate that is dependent on the applied force. By adding different concentrations of DTT and monitoring the kinetics of protein unfolding, we estimated the

relative tension applied by different subtypes of integrins (Figure 6D and E). These kinetic measurements of I27 unfolding allow estimation of the applied integrin forces within FAs. Although, the values are dependent on the unfolding parameters determined by Fernandez and co-workers,[57] this approach provides the only method to infer the applied forces within stable FAs.

## 4. CONCLUSION AND FUTURE OUTLOOK

We present in this Account a new general approach to visualize molecular tension tension applied by cell surface receptors. MTFM demonstrates key advantages over conventional biophysical methods (TFM and SMFS) for mapping cellular traction forces. We envisage that further improvements in MTFM will broaden its scope and will eventually allow this method to become established as one of the workhorse tools in the field of mechanotransduction.

The limitations of FRET probes require the development of alternative force readout strategies. For example, FRET suffers from photobleaching, oxidation, and an upper limit of measured distance of ~10 nm.[58] Compared to organic dyes, quantum dots (QDs) display improved brightness and superior photostability and QD-based MTFM probes may address these challenges.[59] Furthermore, large plasmonic nanoparticles (>20 nm) comprised of gold and silver have also been utilized as spectroscopic rulers.[60] The advantages of these reporters include a stable scattering signal that is orders of magnitude brighter than organic dyes, thus potentially boosting the temporal resolution and enabling long-term force imaging without photobleaching. Another improved readout is the use of PCR-like or ELISA-like amplification strategies.[25] For example, we developed signal amplification strategies to transduce a specific pN force into a chemical reaction. This is akin to a mechanically triggered ELISA or a mechanically triggered PCR reaction. This type of reaction may allow for detection of molecular traction forces using high content imaging.

Unfolding of DNA and protein MTFM probes depends linearly on the logarithm of force loading rate.[16] However, many secondary structures can be unfolded when a small, isometric force (1−5 pN) is applied for sufficient time. For example, early AFM experiments showed that the unfolding force for I27 was greater than 100 pN with pulling speeds of 0.01−0.5 μm/s.[56] In contrast, I27 was shown to unfold when a force of ~ 5.4 pN is held constant for up to 8 hours.[61] To date, the loading rate of cellular contractile forces is still unknown, which makes it less meaningful to compare the absolute value of forces acquired using different classes of probes. Note that the best estimate of receptor forces is likely though the use of the $F_{1/2}$ value defined at equilibrium for DNA hairpins. These values represent a minimum force, as any loading rate would increase the required force for unfolding.

Lastly, developing appropriate chemistry to incorporate MTFM probes with 3D matrices is one of the most urgent and challenging tasks. This new chemistry has to be coupled with ultrasensitive 3D microscopy methods, such as light sheet fluorescence microscopy,[62] to capture receptor forces in an 3D environment. An increasing amount of evidence has demonstrated that cell adhesion and migration are profoundly altered when cells are cultured in a physiological 3D microenvironment versus 2D substrates.[63] In contrast to 2D culture,

natural 3D ECM in tissue consists of a meshwork with fibers and gaps providing complex biochemical and physical cues. Key parameters such as local ligand density, matrix stiffness, porosity and fibril alignment synergistically influence cell mechanics. Therefore, there are many differences in cell behavior in 2D compared to 3D culture.[64,65] For example, it remains unclear that how integrin-mediated focal adhesions or equivalent structures form in a 3D environment and what magnitude of mechanical forces is generated through these structures. Given the simplicity of force quantification using MTFM probes and superior compatibility with any 3D fluorescence imaging technique, it is highly desirable to redesign MTFM probes of facile conjugation chemistry for mechano-imaging of cells in 3D culture.

## Biographical Information

**Yang Liu** graduated from Hunan University (PR China) with a B.S. in Chemistry and received his Ph.D. at Emory University under the guidance of Prof. Khalid Salaita. He is now a postdoctoral researcher in Prof. Taekjip Ha's lab at Johns Hopkins University.

**Kornelia Galior** received her B.S. in Chemistry from Appalachian State University and her Ph.D. at Emory University under the guidance of Prof. Khalid Salaita. She is now a postdoctoral fellow in clinical chemistry at Mayo Clinic.

**Victor Pui-Yan Ma** completed his B.Sc. in Chemistry at Hong Kong Baptist University (Hong Kong), and is currently pursuing his Ph.D. at Emory University under the tutelage of Prof. Khalid Salaita. His current research interest is in the development of force sensing systems to study mechano-regulation of T-cells.

**Khalid Salaita** received his Ph.D. in Chemistry from Northwestern University in 2006 with Prof. Chad A. Mirkin. After a postdoctoral fellowship with Prof. Jay T. Groves at the University of California, Berkeley, he joined Emory University in 2009 where he is currently an Associate Professor of Chemistry and a program faculty of Wallace H. Coulter Department of Biomedical Engineering. His research group is focused on the interface of nanotechnology and cell biology.

## References

(1). Asally M; Kittisopikul M; Rue P; Du Y; Hu Z; Cagatay T; Robinson AB; Lu H; Garcia-Ojalvo J; Suel GM Localized cell death focuses mechanical forces during 3D patterning in a biofilm. Proc. Natl. Acad. Sci. USA 2012, 109, 18891–18896.23012477

(2). Mammoto T; Ingber DE Mechanical control of tissue and organ development. Development 2010, 137, 1407–1420.20388652

(3). Judokusumo E; Tabdanov E; Kumari S; Dustin ML; Kam LC Mechanosensing in T lymphocyte activation. Biophys. J 2012, 102, L5–7.22339876

(4). Brugues A; Anon E; Conte V; Veldhuis JH; Gupta M; Colombelli J; Munoz JJ; Brodland GW; Ladoux B; Trepat X Forces driving epithelial wound healing. Nat. Phys 2014, 10, 683–690.27340423

(5). McBeath R; Pirone DM; Nelson CM; Bhadriraju K; Chen CS Cell shape, cytoskeletal tension, and RhoA regulate stem cell lineage commitment. Dev. Cell 2004, 6, 483–495.15068789

(6). Ingber DE Cellular mechanotransduction: putting all the pieces together again. FASEB J 2006, 20, 811–827.16675838

(7). Schwartz MA Integrins and Extracellular Matrix in Mechanotransduction. Cold Spring Harb. Perspect. Biol 2010, 2, a005066.21084386

(8). Borghi N; Sorokina M; Shcherbakova OG; Weis WI; Pruitt BL; Nelson WJ; Dunn AR E-cadherin is under constitutive actomyosin-generated tension that is increased at cell–cell contacts upon externally applied stretch. Proceedings of the National Academy of Sciences of the United States of America 2012, 109, 12568–12573.22802638

(9). Liu Y; Blanchfield L; Ma VP; Andargachew R; Galior K; Liu Z; Evavold B; Salaita K DNA-based nanoparticle tension sensors reveal that T-cell receptors transmit defined pN forces to their antigens for enhanced fidelity. Proc. Natl. Acad. Sci. USA 2016, 113, 5610–5615.27140637

(10). Wan Z; Chen X; Chen H; Ji Q; Chen Y; Wang J; Cao Y; Wang F; Lou J; Tang Z; Liu W The activation of IgM- or isotype-switched IgG- and IgE-BCR exhibits distinct mechanical force sensitivity and threshold. eLife 2015, 4.

(11). Luca VC; Kim BC; Ge C; Kakuda S; Wu D; Roein-Peikar M; Haltiwanger RS; Zhu C; Ha T; Garcia KC Notch-Jagged complex structure implicates a catch bond in tuning ligand sensitivity. Science 2017, 355, 1320–1324.28254785

(12). Salaita K; Nair PM; Petit RS; Neve RM; Das D; Gray JW; Groves JT Restriction of Receptor Movement Alters Cellular Response: Physical Force Sensing by EphA2. Science 2010, 327, 1380–1385.20223987

(13). Schoen I; Pruitt BL; Vogel V The Yin-Yang of Rigidity Sensing: How Forces and Mechanical Properties Regulate the Cellular Response to Materials. Annu. Rev. Mat. Res 2013, 43, 589–618.

(14). Kong F; Garcia AJ; Mould AP; Humphries MJ; Zhu C Demonstration of catch bonds between an integrin and its ligand. J. Cell Biol 2009, 185, 1275–1284.19564406

(15). Liu B; Chen W; Evavold Brian D.; Zhu C Accumulation of Dynamic Catch Bonds between TCR and Agonist Peptide-MHC Triggers T Cell Signaling. Cell 2014, 157, 357–368.24725404

(16). Evans E Probing the relation between force--lifetime--and chemistry in single molecular bonds. Annu. Rev. Biophys. Biomol. Struct 2001, 30, 105–128.11340054

(17). Bell GI Models for the specific adhesion of cells to cells. Science 1978, 200, 618–627.347575

(18). Bustamante C; Chemla YR; Forde NR; Izhaky D Mechanical processes in biochemistry. Annu. Rev. Biochem 2004, 73, 705–748.15189157

(19). Polacheck WJ; Chen CS Measuring cell-generated forces: a guide to the available tools. Nat. Meth 2016, 13, 415–423.

(20). Hategan A; Law R; Kahn S; Discher DE Adhesively-tensed cell membranes: lysis kinetics and atomic force microscopy probing. Biophys. J 2003, 85, 2746–2759.14507737

(21). Neuman KC; Nagy A Single-molecule force spectroscopy: optical tweezers, magnetic tweezers and atomic force microscopy. Nat. Meth 2008, 5, 491–505.

(22). Stabley DR; Jurchenko C; Marshall SS; Salaita KS Visualizing mechanical tension across membrane receptors with a fluorescent sensor. Nature Methods 2012, 9, 64–67.

(23). Jurchenko C; Salaita KS Lighting Up the Force: Investigating Mechanisms of Mechanotransduction Using Fluorescent Tension Probes. Mol. Cell. Biol 2015, 35, 2570–2582.26031334

(24). Ma VPY; Liu Y; Blanchfield L; Su HQ; Evavold BD; Salaita K Ratiometric Tension Probes for Mapping Receptor Forces and Clustering at Intermembrane Junctions. Nano Lett 2016, 16, 4552–4559.27192323

(25). Ma VP; Liu Y; Yehl K; Galior K; Zhang Y; Salaita K Mechanically Induced Catalytic Amplification Reaction for Readout of Receptor-Mediated Cellular Forces. Angew. Chem. Int. Ed 2016, 55, 5488–5492.

(26). Liphardt J; Onoa B; Smith SB; Tinoco I; Bustamante C Reversible unfolding of single RNA molecules by mechanical force. Science 2001, 292, 733–737.11326101

(27). Potisek SL; Davis DA; Sottos NR; White SR; Moore JS Mechanophore-linked addition polymers. J. Am. Chem. Soc 2007, 129, 13808–13809.17958363

(28). Choi CL; Koski KJ; Sivasankar S; Alivisatos AP Strain-Dependent Photoluminescence Behavior of CdSe/CdS Nanocrystals with Spherical, Linear, and Branched Topologies. Nano Lett 2009, 9, 3544–3549.19678687

(29). Shroff H; Reinhard BM; Siu M; Agarwal H; Spakowitz A; Liphardt J Biocompatible Force Sensor with Optical Readout and Dimensions of 6 nm3. Nano Lett 2005, 5, 1509–1514.16178266

(30). Morimatsu M; Mekhdjian AH; Adhikari AS; Dunn AR Molecular Tension Sensors Report Forces Generated by Single Integrin Molecules in Living Cells. Nano Lett 2013, 13, 3985–3989.23859772

(31). Zhang Y; Ge C; Zhu C; Salaita K DNA-based digital tension probes reveal integrin forces during early cell adhesion. Nat. Commun 2014, 5, 5167.25342432

(32). Galior K; Liu Y; Yehl K; Vivek S; Salaita K Titin-Based Nanoparticle Tension Sensors Map High-Magnitude Integrin Forces within Focal Adhesions. Nano Lett 2016, 16, 341–348.26598972

(33). Konen J; Summerbell E; Dwivedi B; Galior K; Hou Y; Rusnak L; Chen A; Saltz J; Zhou W; Boise LH; Vertino P; Cooper L; Salaita K; Kowalski J; Marcus AI Image-guided genomics of phenotypically heterogeneous populations reveals vascular signalling during symbiotic collective cancer invasion. Nat. Commun 2017, 8, 15078.28497793

(34). Tinoco I; Bustamante C The effect of force on thermodynamics and kinetics of single molecule reactions. Biophys. Chem 2002, 101, 513–533.12488024

(35). Bustamante Carlos; Chemla Yann R; Forde, a Nancy R; Izhaky D Mechanical Processes in Biochemistry. Annu. Rev. Biochem 2004, 73, 705–748.15189157

(36). Woodside MT; Behnke-Parks WM; Larizadeh K; Travers K; Herschlag D; Block SM Nanomechanical measurements of the sequence-dependent folding landscapes of single nucleic acid hairpins. Proc. Natl. Acad. Sci. USA 2006, 103, 6190–6195.16606839

(37). De Gennes P Conformations of polymers attached to an interface. Macromolecules 1980, 13, 1069–1075.

(38). Bouchiat C; Wang M; Allemand JF; Strick T; Block S; Croquette V Estimating the persistence length of a worm-like chain molecule from force-extension measurements. Biophysical Journal 1999, 76, 409–413.9876152

(39). Liu Y; Yehl K; Narui Y; Salaita K Tension Sensing Nanoparticles for Mechano-Imaging at the Living/Nonliving Interface. J. Am. Chem. Soc 2013, 135, 5320–5323.23495954

(40). Marras SA; Kramer FR; Tyagi S Efficiencies of fluorescence resonance energy transfer and contact-mediated quenching in oligonucleotide probes. Nucleic Acids Res 2002, 30, e122.12409481

(41). Yun C; Javier A; Jennings T; Fisher M; Hira S; Peterson S; Hopkins B; Reich N; Strouse G Nanometal surface energy transfer in optical rulers, breaking the FRET barrier. J. Am. Chem. Soc 2005, 127, 3115–3119.15740151

(42). Breshike CJ; Riskowski RA; Strouse GF Leaving Forster Resonance Energy Transfer Behind: Nanometal Surface Energy Transfer Predicts the Size-Enhanced Energy Coupling between a Metal Nanoparticle and an Emitting Dipole. J. Phys. Chem C 2013, 117, 23942–23949.

(43). Jurchenko C; Chang Y; Narui Y; Zhang Y; Salaita, Khalid S. Integrin-Generated Forces Lead to Streptavidin-Biotin Unbinding in Cellular Adhesions. Biophysical Journal 2014, 106, 1436–1446.24703305

(44). Chang Y; Liu Z; Zhang Y; Galior K; Yang J; Salaita K A General Approach for Generating Fluorescent Probes to Visualize Piconewton Forces at the Cell Surface. J. Am. Chem. Soc 2016, 138, 2901–2904.26871302

(45). Morimatsu M; Mekhdjian AH; Chang AC; Tan SJ; Dunn AR Visualizing the Interior Architecture of Focal Adhesions with High-Resolution Traction Maps. Nano Lett 2015, 15, 2220–2228.25730141

(46). Kapp TG; Rechenmacher F; Neubauer S; Maltsev O; Cavalcanti-Adam EA; Zarka R; Reuning U; Notni J; Wester H-J; Mas-Moruno C; Spatz JP; Geiger B; Kessler H A Comprehensive Evaluation of the Activity and Selectivity Profile of Ligands for RGD-binding Integrins. Sci. Rep 2017, 7, 39805.28074920

(47). Stone JD; Chervin AS; Kranz DM T-cell receptor binding affinities and kinetics: impact on T-cell activity and specificity. Immunology 2009, 126, 165–176.19125887

(48). Wang X; Ha T Defining Single Molecular Forces Required to Activate Integrin and Notch Signaling. Science 2013, 340, 991–994.23704575

(49). Blakely BL; Dumelin CE; Trappmann B; McGregor LM; Choi CK; Anthony PC; Duesterberg VK; Baker BM; Block SM; Liu DR; Chen CS A DNA-based molecular probe for optically reporting cellular traction forces. Nat. Meth 2014, 11, 1229–1232.

(50). Wang X; Rahil Z; Li ITS; Chowdhury F; Leckband BE; Chemla YR; Ha T Constructing modular and universal single molecule tension sensor using protein G to study mechano-sensitive receptors. Sci. Rep 2016, 6, 21584.26875524

(51). Xue Y; Li X; Li H; Zhang W Quantifying thiol-gold interactions towards the efficient strength control. Nat. Commun 2014, 5, 4348.25000336

(52). Liu Y; Medda R; Liu Z; Galior K; Yehl K; Spatz JP; Cavalcanti-Adam EA; Salaita K Nanoparticle Tension Probes Patterned at the Nanoscale: Impact of Integrin Clustering on Force Transmission. Nano Lett 2014, 14, 5539–5546.25238229

(53). Changede R; Sheetz M Integrin and cadherin clusters: A robust way to organize adhesions for cell mechanics. BioEssays 2017, 39, 1–12.

(54). Chillakuri CR; Sheppard D; Lea SM; Handford PA Notch receptor–ligand binding and activation: Insights from molecular studies. Semin. Cell Dev. Biol 2012, 23, 421–428.22326375

(55). Manz BN; Groves JT Spatial organization and signal transduction at intercellular junctions. Nat. Rev. Mol. Cell. Biol 2010, 11, 342–352.20354536

(56). Rief M; Gautel M; Oesterhelt F; Fernandez JM; Gaub HE Reversible unfolding of individual titin immunoglobulin domains by AFM. Science 1997, 276, 1109–1112.9148804

(57). Wiita AP; Ainavarapu SRK; Huang HH; Fernandez JM Force-dependent chemical kinetics of disulfide bond reduction observed with single-molecule techniques. Proc. Natl. Acad. Sci. USA 2006, 103, 7222–7227.16645035

(58). Roy R; Hohng S; Ha T A practical guide to single-molecule FRET. Nature Methods 2008, 5, 507–516.18511918

(59). Resch-Genger U; Grabolle M; Cavaliere-Jaricot S; Nitschke R; Nann T Quantum dots versus organic dyes as fluorescent labels. Nature Methods 2008, 5, 763–775.18756197

(60). Xiong B; Huang Z; Zou H; Qiao C; He Y; Yeung ES Single Plasmonic Nanosprings for Visualizing Reactive-Oxygen-Species-Activated Localized Mechanical Force Transduction in Live Cells. ACS Nano 2017, 11, 541–548.28038314

(61). Chen H; Yuan G; Winardhi RS; Yao M; Popa I; Fernandez JM; Yan J Dynamics of Equilibrium Folding and Unfolding Transitions of Titin Immunoglobulin Domain under Constant Forces. J. Am. Chem. Soc 2015, 137, 3540–3546.25726700

(62). Chen B-C; Legant WR; Wang K; Shao L; Milkie DE; Davidson MW; Janetopoulos C; Wu XS; Hammer JA; Liu Z; English BP; Mimori-Kiyosue Y; Romero DP; Ritter AT; Lippincott-Schwartz J; Fritz-Laylin L; Mullins RD; Mitchell DM; Bembenek JN; Reymann A-C; Böhme R; Grill SW; Wang JT; Seydoux G; Tulu US; Kiehart DP; Betzig E Lattice light-sheet microscopy: Imaging molecules to embryos at high spatiotemporal resolution. Science 2014, 346.

(63). Doyle AD; Yamada KM Mechanosensing via cell-matrix adhesions in 3D microenvironments. Exp. Cell Res 2016, 343, 60–66.26524505

(64). Dalby MJ; Gadegaard N; Oreffo ROC Harnessing nanotopography and integrin-matrix interactions to influence stem cell fate. Nat. Mater 2014, 13, 558–569.24845995

(65). Schulte C; Ripamonti M; Maffioli E; Cappelluti MA; Nonnis S; Puricelli L; Lamanna J; Piazzoni C; Podestà A; Lenardi C; Tedeschi G; Malgaroli A; Milani P Scale Invariant Disordered Nanotopography Promotes Hippocampal Neuron Development and Maturation with Involvement of Mechanotransductive Pathways. Front. Cell. Neurosci 2016, 10.

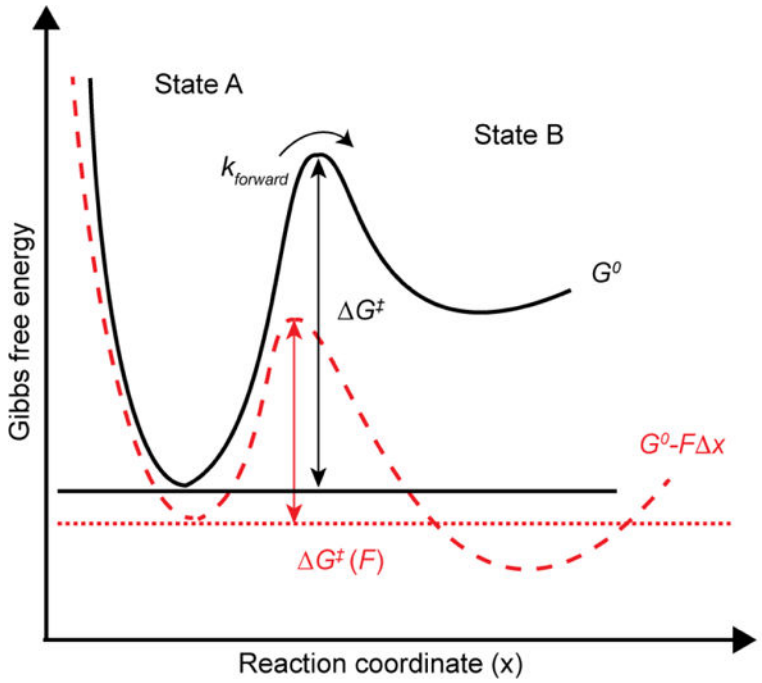


**Figure 1. Mechanical unfolding of biomolecules.**

Free energy landscape of a two-state model representative of a biomolecule adopting two states (A, B) separated by an energy barrier.

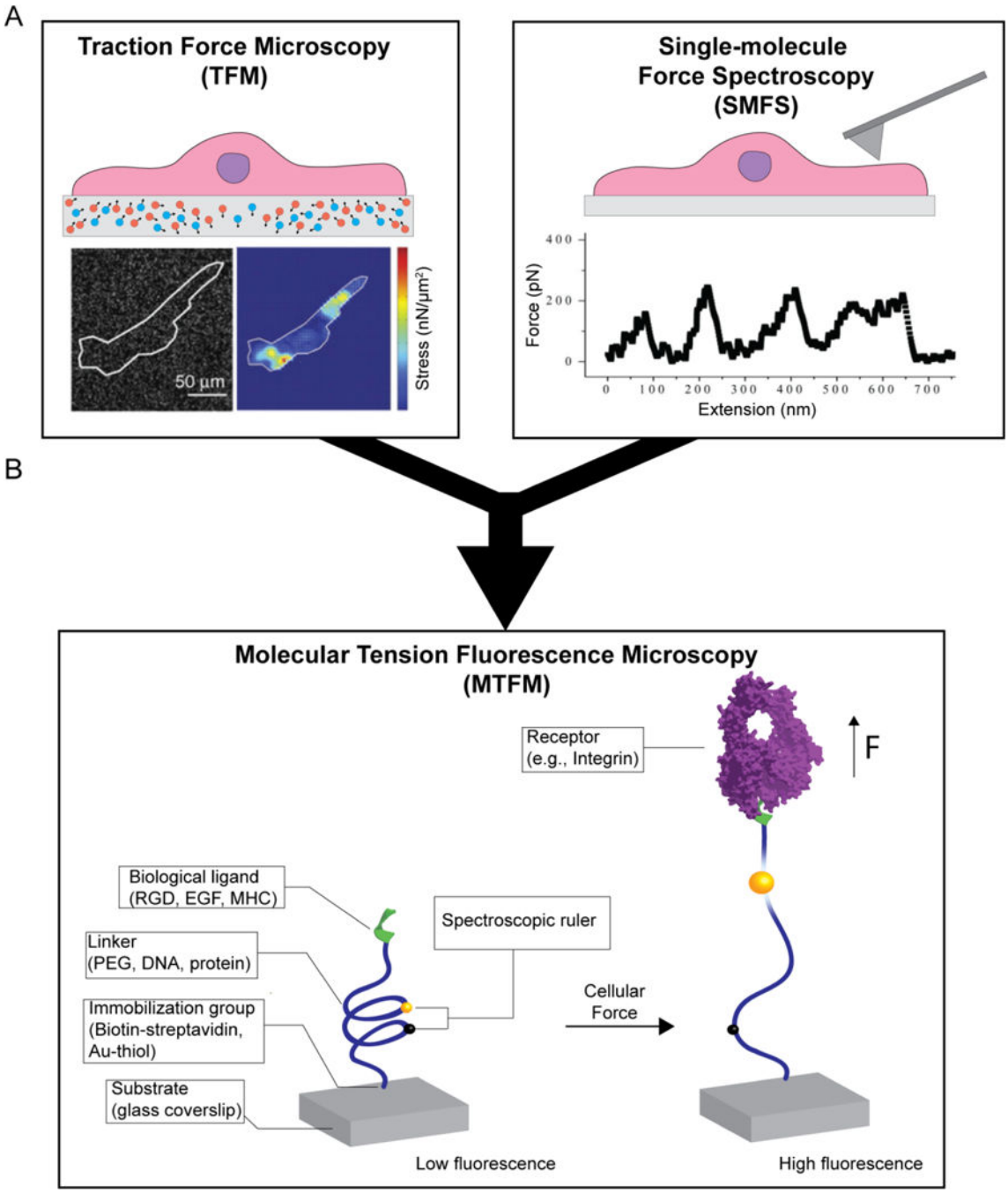


**Figure 2. Schematic of current technologies to image cell forces.**

(A) Scheme depicting traction force microscopy (TFM) and single-molecule force spectroscopy (SMFS). Adapted with permission from ref 19. Copyright (2016) Nature Publishing Group, and ref 20. Copyright (2003) Elsevier. (B) Simplified diagram that shows how tension probes report on cell forces.

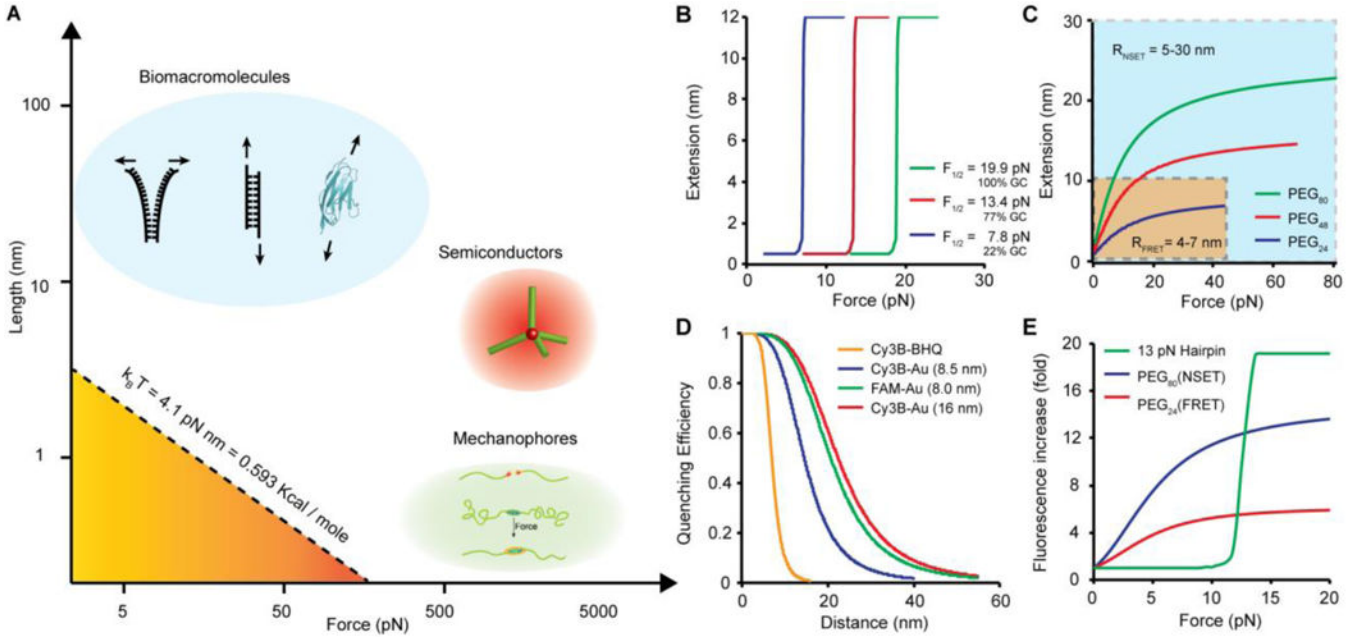


**Figure 3. Force-extension relation for different molecular force probes.**

(A) Plot showing the force-extension relationship of biomolecules [blue: DNA duplex and titin immunoglobulin I27 domain (PDB ID: 1TIT)] used in MTFM; semiconductor tetrapod (red) and mechanophores (green). The dashed line corresponds to the mechanical work (product of force multiplied by deformation distance) that is equivalent to thermal energy ($k_B$T, at room temperature). The stability of tension probes is greater than $k_B$T and tuned to probe different processes. **(**B**)** Plot showing the expected force-extension curve for DNA hairpins of different GC contents at 25°C. The plots were generated using eq. 2 which describes the unfolding probabilities of DNA as a function of applied forces. (C) Theoretical plot showing the force responses of PEG linkers as a function of PEG length distance. The yellow region highlights the range of extensions that can be detected by fluorescence resonance energy transfer (FRET), while the blue region highlights the range of distances probed by nanometal surface energy transfer (NSET). (D) Plot showing the NSET quenching efficiency as a function of PEG extension with different energy transfer mechanisms (parenthesis indicates the radius of AuNP). Experimental data re-plotted from ref 39 (E) Plot comparing the fold increase of donor fluorescence as a function of tension applied to different probes.

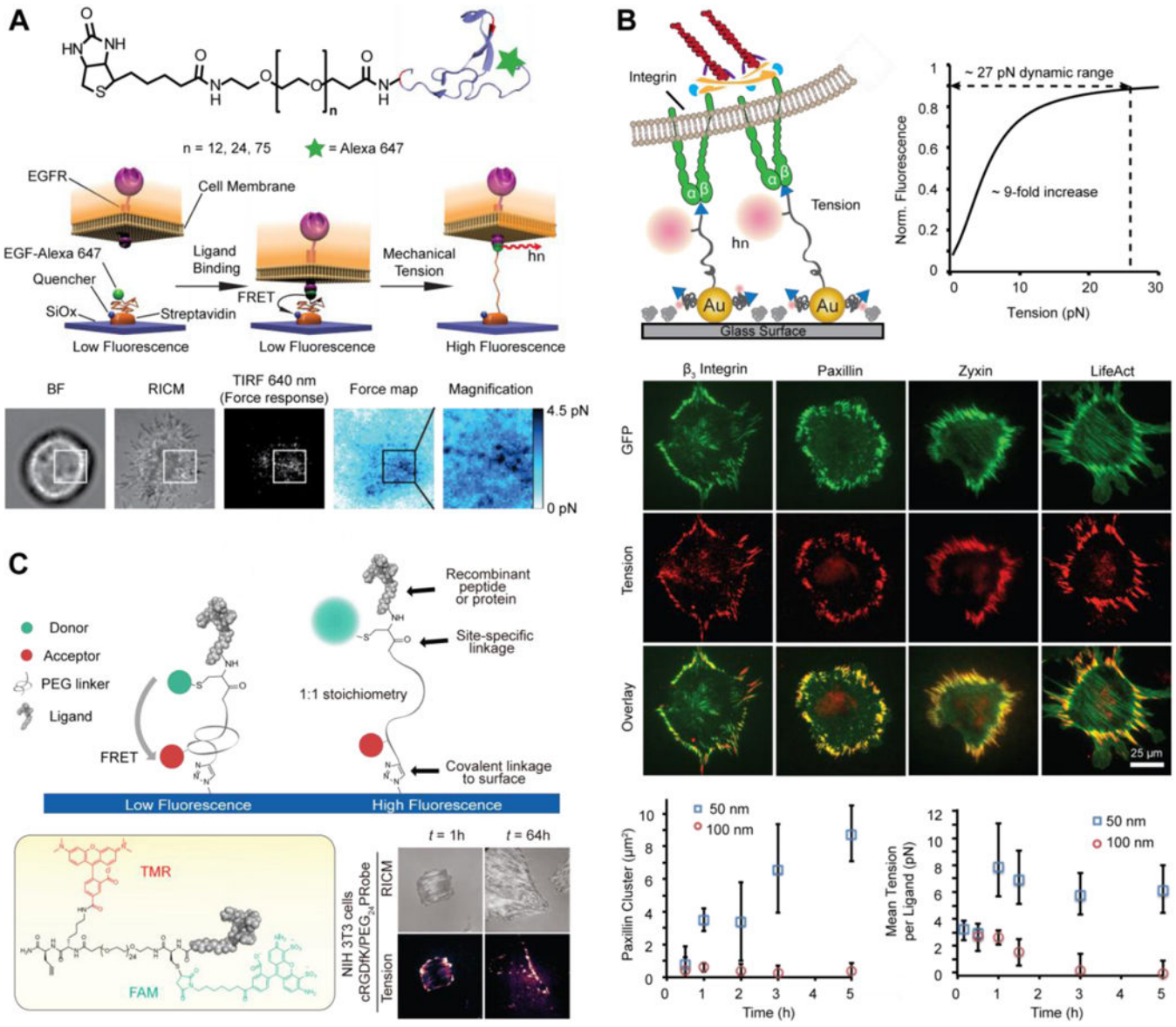


**Figure 4. PEG-based MTFM Probes.**

(A) Schematic of the PEG tension sensor, comprised of a PEG polymer flanked with a fluorescently labeled (Alexa Fluor 647) EGF ligand and a biotin moiety for surface immobilization (Top). When EGFR exerts a force on its ligand, the flexible PEG linker extends. The displacement of the EGF ligand results in an increase in the measured fluorescence intensity, thus reporting the transmission of mechanical tension through the EGF-EGFR complex (Middle). Representative brightfield, RICM and fluorescence response for a cell engaged to an EGF-PEG24 force sensor surface. The sensor fluorescence response was converted into a force map by using the extended WLC model (eq. 3) for PEG24 (Bottom) Adapted with the permission from ref 22. Copyright 2013 Nature publishing group. (B) Schematic showing the expected mechanism of how cell-generated forces activate the AuNP tension probe. Theoretical plot showing the change in fluorescence as a function of applied tension based on combining the WLC (eq. 3) and NSET models. The

dynamic range of the probe corresponds to quenching efficiency values ranging from 90 to 10%. Representative TIRFM-488 (GFP channel, green) and Cy3B epifluorescence (integrin-tension channel, red) images of NIH/3T3 fibroblast cells cultured on randomly arranged AuNP sensor substrates for 1−2 h. The cells were transiently transfected to express GFP β3-integrin, paxillin, zyxin, and LifeAct, and this signal was found to colocalize with the integrin tension signal. Plot of GFP paxillin cluster size (which is indicative of FA size) as a function of time for n = 10 cells. The plots show the steady increase in FA size and tension over 5 h after cell seeding on the 50 nm-spaced substrate, which is in contrast to the 100 nm spaced substrate, which shows limited FA maturation. Adapted from ref 52. Copyright 2014 American Chemical Society. (C) Synthetic scheme for generating ligand-general MTFM Probes. RICM and fluorescence images showing the cell−substrate contact zone along with a map of integrin tension at 1h and 64 h. Adapted from ref 44. Copyright 2016 American Chemical Society.

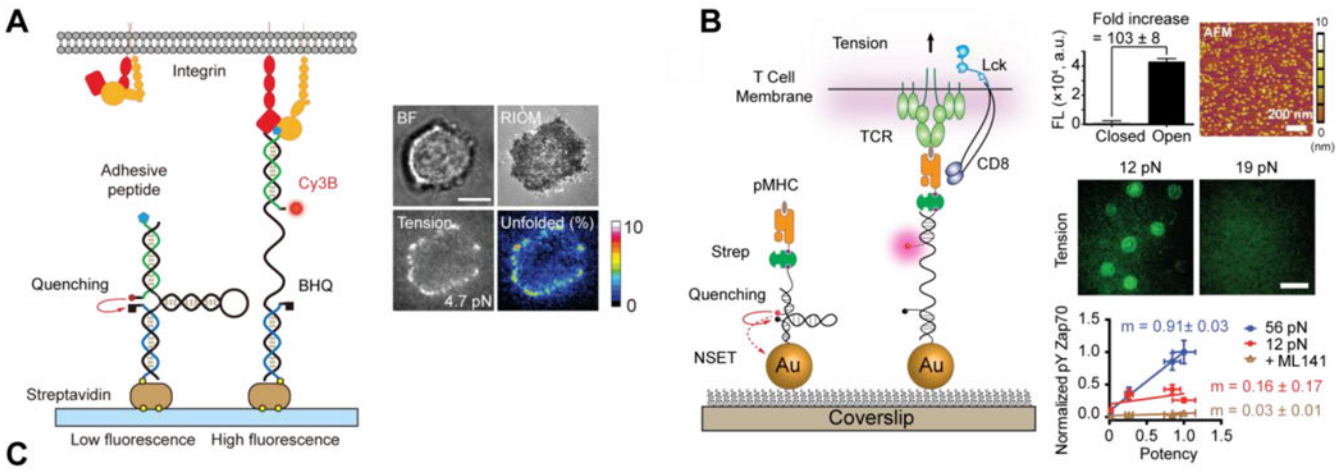


C

| GC content | 22% | 35% | 77% | 100% | 100% |
|---|---|---|---|---|---|
| Total hairpin size (mer) | 25 | 44 | 25 | 28 | 44 |
| Loop size (mer) | 7 | 4 | 7 | 4 | 4 |
| Calculated $F_{1/2}$ [a] | 7.8 pN | 12 pN | 13.4 pN | 20.2 pN | 19.9 pN |
| Calibrated | 4.7 pN[b] | Not measured | Not measured | 13.1 pN[c] | 19.3 pN[d] |

a : T = 25 °C, [$Na^+$] = 137.3 mM, [$Mg^{2+}$] = 0.8 mM
b, c : calibrated using BFP ( reference 31)
d : calibrated using optical trap ( reference 36 )

**Figure 5.**

(A) Schematic of the DNA-based tension sensor, which is comprised of an anchor strand immobilized onto a surface (blue), a hairpin strand that unfolds under sufficient tension (black) and a ligand strand presenting an adhesive peptide (green). At the apposing termini of the ligand and anchoring strands, a fluorophore and quencher were coupled to report the force-induced unfolding of the hairpin (left). Table summarizes the calculated and measured $F_{1/2}$ values, GC content and the calculated free energy of hybridization of all hairpins used (top right). Representative brightfield, RICM and tension (4.7 pN) images show the initial stage of cell spreading and adhesion (bottom right). Adapted with permission from ref 31. Copyright 2014 Nature publishing group. (B) Schematic of DNA-based AuNP sensor for mapping TCR-mediated tension. The fluorescence of the Cy3B dye (pink dot) is dequenched upon mechanical unfolding of the hairpin, which separates the dye from the black hole quencher 2 (BHQ2, block dot) and AuNP surface (left). Plot shows a 103 ± 8-fold increase in fluorescence on the opening of hairpins and AFM image shows the immobilized AuNP sensors on a glass coverslip (top right). Representative tension images of OT-1 cells cultured on tension probe surfaces modified with N4 pMHC show differential force response on 12 and 19 pN probes (middle right). Plot of pYZap70 levels in response to ligands with increasing potency under physical or chemical perturbations. The slope (m) indicates the T-cell specificity to different ligands (bottom right). Adapted with permission from ref 9. Copyright 2016 National Academy of Sciences, USA. (C) Table showing a list of DNA hairpin probes used for tension sensing.

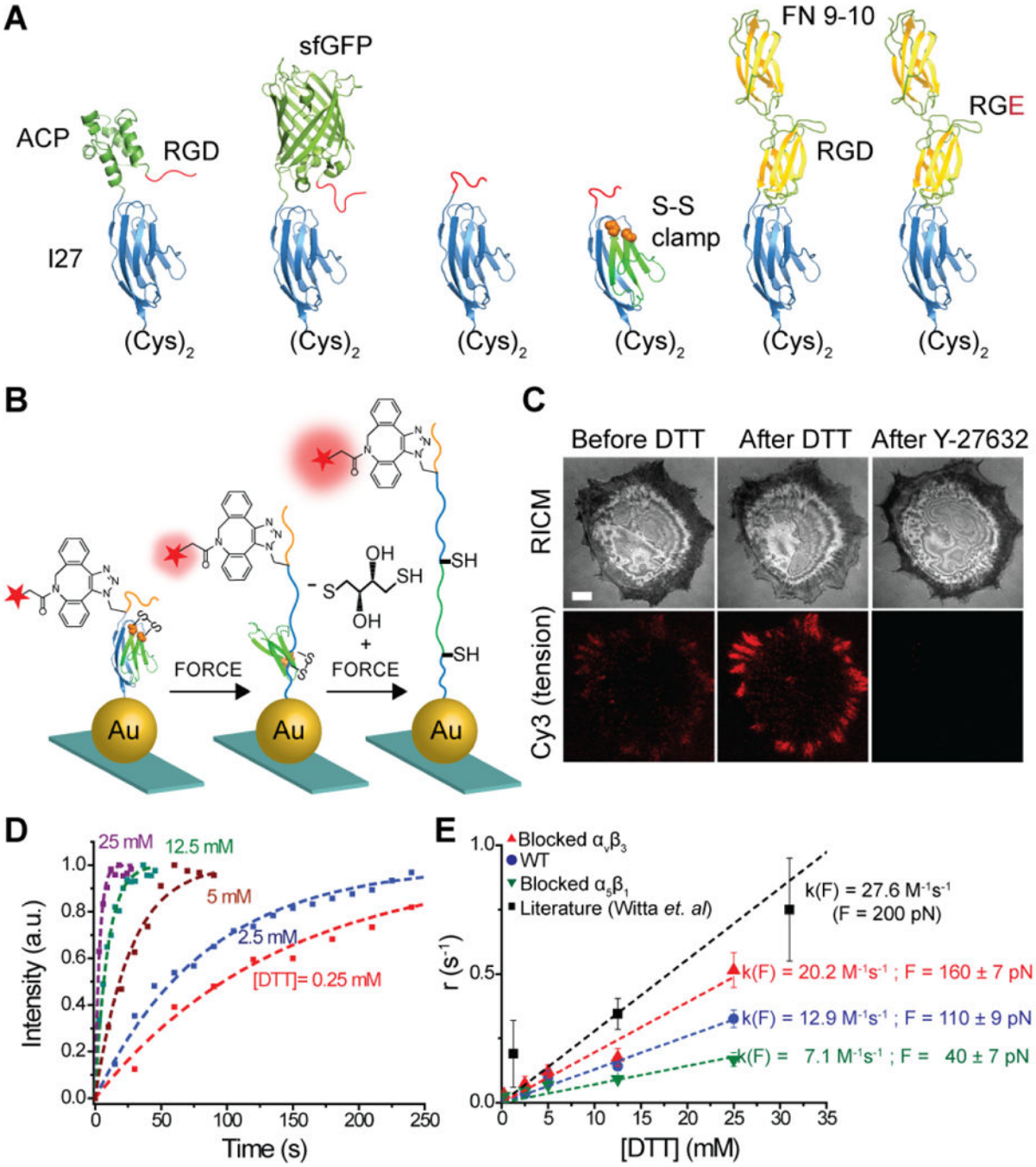


**Figure 6.**

(A) Schematic showing a series of I27 based tension probes with different fluorescent reporters and ligands. (B) Schematic illustration of disulfide clamped I27 tension sensor. When cells apply tension to the clamped MTFM sensor, I27 is stretched to the position of the disulfide clamp, resulting in solvent exposure of the disulfide. I27 can be further mechanically extended only in the presence of reducing agent, such as DTT. (C) Representative RICM and clamped I27 tension signal for REF cells incubated onto the sensor surface for 2 h before and after treatment with 0.25 mM DTT for 10 min, and then

after treatment with Y-27632 (40 μM) for 30 min. Scale bar, 10 μm. (D) Representative kinetic plots showing an increase in fluorescence tension signal at different DTT concentrations. Dashed lines represent single-exponential fits used to determine reduction rate. (E) Plot of the rate of disulfide reduction as a function of [DTT] for REF cells (blue), REF cells blocked with $\alpha_v\beta_3$ (red), and $\alpha_5\beta_1$ antibodies (green). Adapted from ref 32. Copyright 2016 American Chemical Society.

**Table 1.**

A comparison of the advantages and disadvantages of polymer network deformation techniques (TFM), single-molecule force spectroscopy (SMFS) and molecular tension probes.

| | Traction force microscopy/ micro-post array detectors | Single Molecule methods (AFM/ BFP/ Tweezers) | Molecular Tension Probes |
|---|---|---|---|
| **Force sensitivity** | *Ensemble (nN)* | *pN* | *pN* |
| **Temporal resolution** | *~sec* | *~msec* | *~msec* |
| **Spatial resolution** | *~1 μm* | *N/A* | *~20 nm*[a] |
| **Throughput** | *High* | *Low* | *High* |

[a] with super-resolution fluorescence microscopy